

# Exploratory Analysis of Peripheral Pharmacodynamic Biomarkers After Sitravatinib and Tislelizumab in Advanced Solid Tumors: SAFFRON-103

FPN: 44P presented at ESMO IO, Geneva, Switzerland, December 6-8, 2023

Yi-Long Wu,<sup>1</sup> Bo Gao,<sup>2</sup> Jeffrey C Goh,<sup>3</sup> Jun Zhao,<sup>4</sup> Zhiyong Ma,<sup>5</sup> Jiwei Cui,<sup>6</sup> Xinmin Yu,<sup>7</sup> Dingzhi Huang,<sup>8</sup> Daphne Day,<sup>9</sup> Mark Voskoboinik,<sup>10</sup> Qian Chu,<sup>11</sup> Qing Zhou,<sup>1</sup> Michael Millward,<sup>12</sup> Hongming Pan,<sup>13</sup> Meili Sun,<sup>14</sup> Yanyan Peng,<sup>15</sup> Mo Liu,<sup>16</sup> Tian Tian,<sup>17</sup> Hui Li,<sup>18</sup> Jun Guo<sup>19</sup>

<sup>1</sup>Guangdong Lung Cancer Institute, Guangdong Provincial People's Hospital (Guangdong Academy of Medical Sciences), Southern Medical University, Guangzhou, China; <sup>2</sup>Department of Medical Oncology, Blacktown Cancer and Haematology Centre, Sydney, Australia; <sup>3</sup>Department of Medical Oncology, Icon Cancer Foundation, Brisbane, Australia; <sup>4</sup>Key Laboratory of Carcinogenesis and Translational Research (Ministry of Education), Department of Thoracic Oncology, Peking University Cancer Hospital and Institute, Beijing, China; <sup>5</sup>Department of Respiratory Medicine, Henan Cancer Hospital/Affiliated Cancer Hospital of Zhengzhou University, Zhengzhou, China; <sup>6</sup>Department of Oncology, The First Bethune Hospital of Jilin University, Changchun, China; <sup>7</sup>Department of Medical Oncology, Zhejiang Cancer Hospital, Hangzhou, China; <sup>8</sup>Department of Thoracic Oncology, Tianjin Medical University Cancer Institute and Hospital, Tianjin, China; <sup>9</sup>Department of Oncology, Monash Health and Monash University, Clayton, Australia; <sup>10</sup>Department of Oncology, The Alfred Hospital, Melbourne, Australia; <sup>11</sup>Department of Oncology, Tongji Hospital, Tongji Medical College, Huazhong University of Science and Technology, Wuhan, China; <sup>12</sup>Linear Clinical Research and University of Western Australia, Perth, Australia; <sup>13</sup>Department of Medical Oncology, Sir Run Run Shaw Hospital, College of Medicine, Zhejiang University, Hangzhou, China; <sup>14</sup>Department of Oncology Internal Medicine, Jinan Central Hospital Affiliated to Shandong University, Jinan, China; <sup>15</sup>Biomarkers, BeiGene (Shanghai) Co., Ltd., Shanghai, China; <sup>16</sup>Bioinformatics, BeiGene (Beijing) Co., Ltd., Beijing, China; <sup>17</sup>Global Statistics, BeiGene (Beijing) Co., Ltd., Beijing, China; <sup>18</sup>Research and Development, BeiGene (Shanghai) Co., Ltd., Shanghai, China; <sup>19</sup>Department of Urology and Melanoma, Peking University Cancer Hospital & Institute, Beijing, China. \*Presenting author.



## Conclusions

Following treatment with sitravatinib plus tislelizumab, patients with advanced solid tumors experienced significant and consistent increases in vascular endothelial growth factor (VEGFA) levels and decreases in soluble vascular endothelial growth factor receptor 2 (sVEGFR2) levels, demonstrating the on-target anti-angiogenesis effect of sitravatinib.

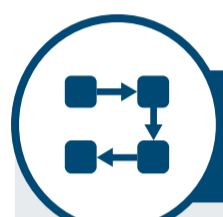
The decrease in granulocyte-like myeloid derived suppressor cells (G-MDSCs) and monocytes in peripheral blood indicates a potential immune-modulating role for sitravatinib with tislelizumab in advanced solid tumors.



## Background

Sitravatinib is an oral spectrum-selective tyrosine kinase inhibitor targeting TAM (TYRO3, AXL, MER) and split tyrosine-kinase domain-containing receptors (VEGFR2, KIT).<sup>1</sup> Tislelizumab, an anti-PD-1 antibody engineered to minimize binding to FcγR on macrophages,<sup>2</sup> has shown clinical activity in patients with advanced solid tumors.<sup>3</sup>

There are few studies investigating the pharmacodynamic biomarkers of sitravatinib and its mechanism of action. Here, we present an exploratory analysis of pharmacodynamic biomarkers in SAFFRON-103 (NCT03666143), a phase 1b study investigating treatment with sitravatinib plus tislelizumab in patients with advanced solid tumors.



## Methods

- This open-label, multicenter, single-arm, nonrandomized phase 1b SAFFRON-103 study enrolled patients with advanced solid tumors, including nonsquamous (nsq) non-small cell lung cancer (NSCLC), squamous (sq) NSCLC, melanoma, or ovarian cancer. The study design has been previously described<sup>4</sup>
- Peripheral blood samples were collected prior to sitravatinib dosing at Cycle (C) 1 Day (D) 1, C2D1, and C3D1, to investigate changes in cytokines (Meso Scale Discovery multiplexing), plasma proteins (enzyme-linked immunosorbent assay), and immune cell populations (fluorescence-activated cell sorting)
- Generalized linear mixed models were used to estimate fold changes in biomarker expression; Wald tests were used to generate *P*-values



## Prognosis Effect

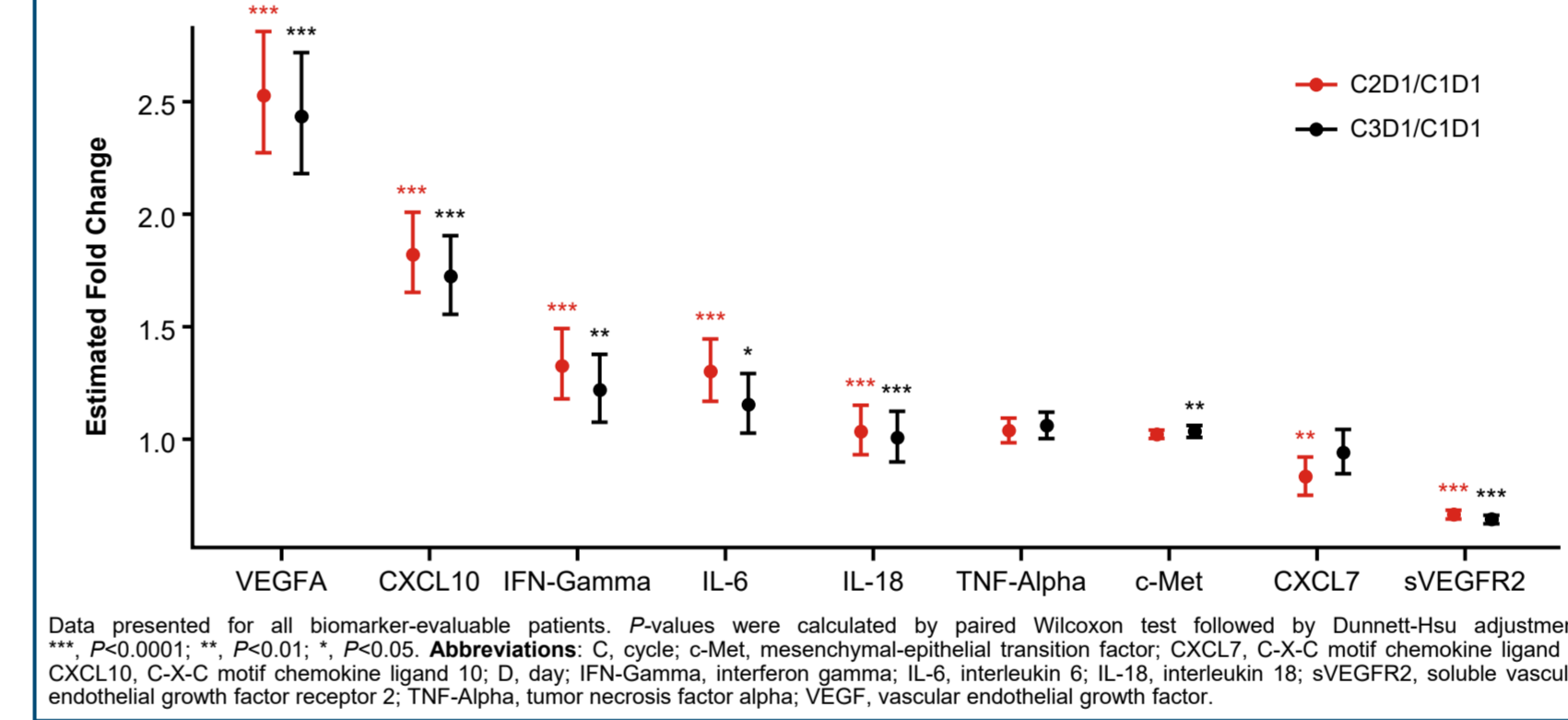
- In Type III tests of fixed effects, changes in VEGFA (increased: odds ratio [OR]=4.67, *P*=0.0005) and monocytes (decreased: OR=5.82, *P*<0.0001) after treatment (C2D1/C1D1) were associated with improved objective response rates
- A Wald test of association between overall survival (OS) and individual biomarkers demonstrated a significant correlation between poor OS and IL-6 (*P*=0.0118), IL-8 (*P*=0.0285), and TNFα (*P*=0.0191)
- VEGFA, sVEGFR2, IFNγ, IL-18, and soluble c-Met levels were not significantly associated with prognosis of advanced solid tumors

Table 1. Patient Baseline Characteristics

	Biomarker-Evaluable Population		Overall Population (N=216)
	Proteins/Cytokines (n=186)	Immune Cells (n=113)	
Age, mean (SD)	60.00 (10.89)	59.15 (11.41)	60.16 (11.03)
Male, n (%)	102 (54.8)	64 (56.6)	113 (52.3)
Tumor type, <sup>a</sup> n (%)			
Melanoma	22 (11.8)	12 (10.6)	25 (11.6)
Nsq NSCLC	60 (32.3)	44 (38.9)	68 (31.5)
Sq NSCLC	48 (25.8)	23 (20.4)	54 (25.0)
Ovarian cancer	54 (29.0)	28 (24.8)	63 (29.2)
PD-L1 score, n (%)			
<1	54 (29.0)	39 (34.5)	60 (27.8)
≥1	80 (43.0)	30 (26.5)	92 (42.6)
Unknown	52 (28.0)	44 (38.9)	64 (29.6)

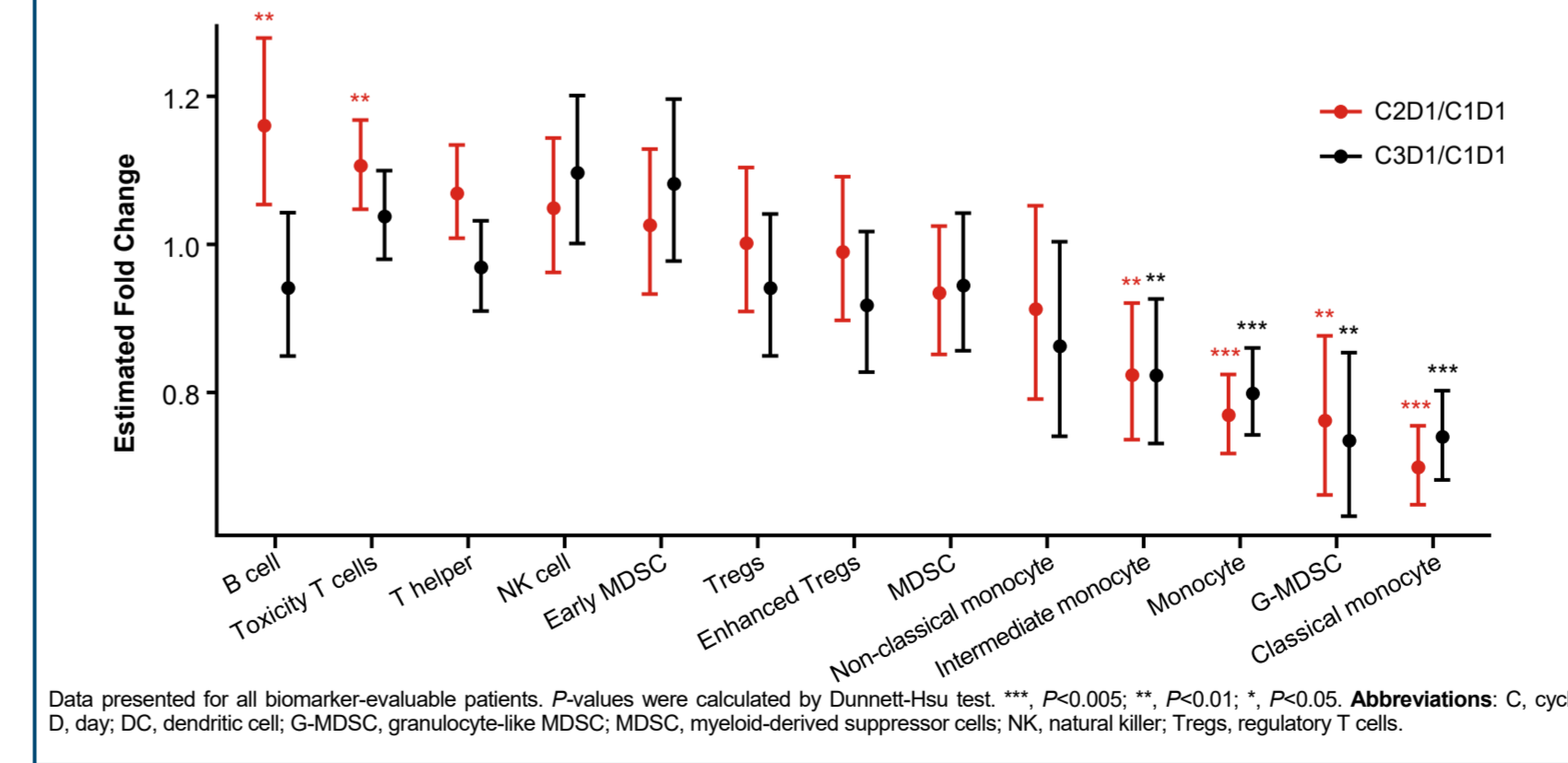
<sup>a</sup>Six patients with renal cell carcinoma were included in the overall population (two patients evaluated for proteins/cytokines, all six evaluated for immune cells). Abbreviations: NSCLC, non-small cell lung cancer; nsq, nonsquamous; PD-L1, programmed death-ligand 1; SD, standard deviation; sq, squamous.

Figure 1. Estimated Fold Change of Soluble Proteins and Cytokines at C2D1 and C3D1 Versus C1D1



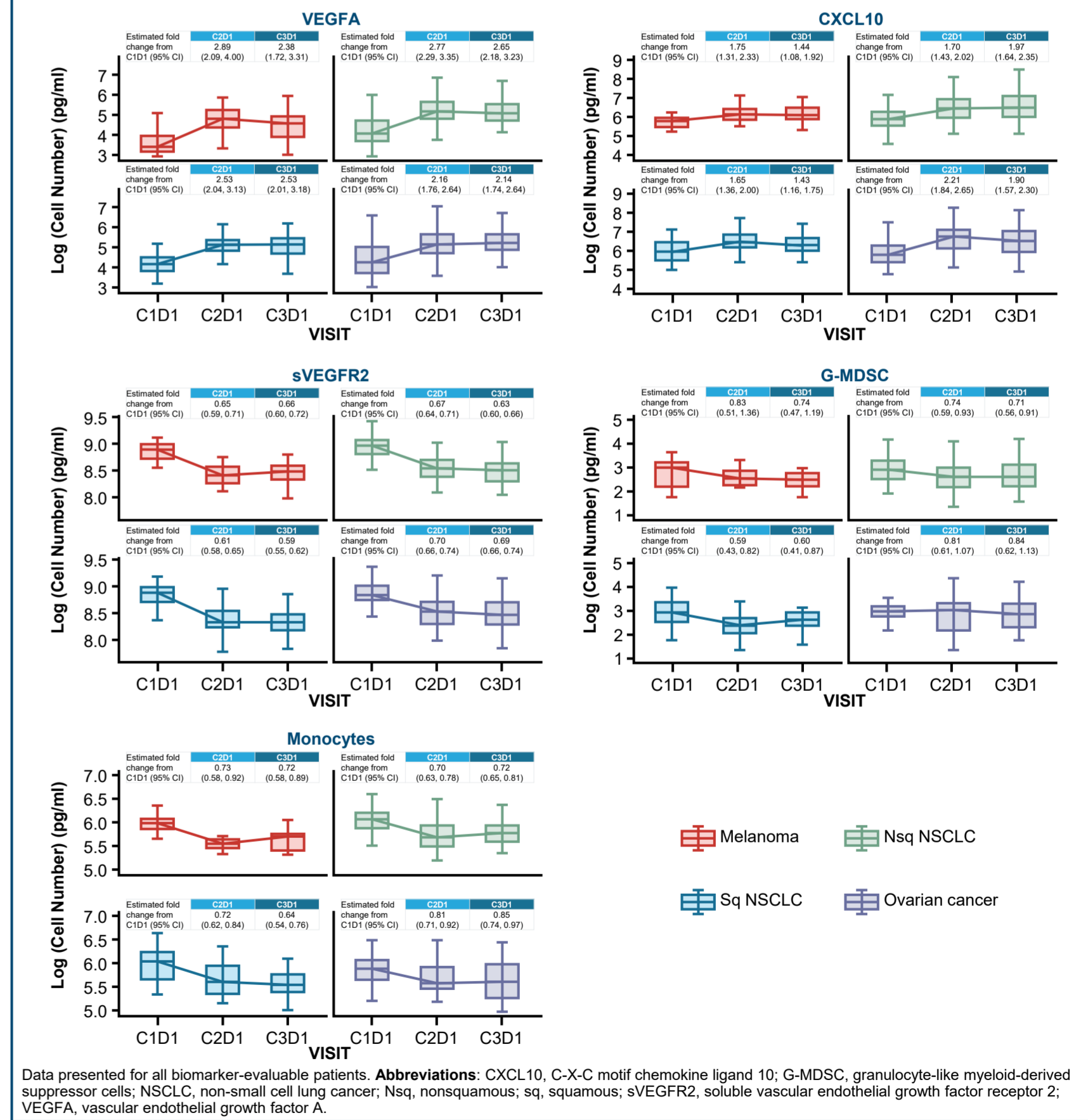
Data presented for all biomarker-evaluable patients. *P*-values were calculated by paired Wilcoxon test followed by Dunnett-Hsu adjustment. \*\*\*, *P*<0.0001; \*\*, *P*<0.01; \*, *P*<0.05. Abbreviations: C, cycle; c-Met, mesenchymal-epithelial transition factor; CXCL7, C-X-C motif chemokine ligand 7; CXCL10, C-X-C motif chemokine ligand 10; D, day; IFN-Gamma, interferon gamma; IL-6, interleukin 6; IL-18, interleukin 18; sVEGFR2, soluble vascular endothelial growth factor receptor 2; TNF-Alpha, tumor necrosis factor alpha; VEGF, vascular endothelial growth factor.

Figure 2. Estimated Fold Change of Immune Cells at C2D1 and C3D1 Versus C1D1



Data presented for all biomarker-evaluable patients. *P*-values were calculated by Dunnett-Hsu test. \*\*\*, *P*<0.0005; \*\*, *P*<0.01; \*, *P*<0.05. Abbreviations: C, cycle; D, day; DC, dendritic cell; G-MDSC, granulocyte-like MDSC; MDSC, myeloid-derived suppressor cells; NK, natural killer; Tregs, regulatory T cells.

Figure 3. Changes in Biomarker Levels Across Tumor Types



Data presented for all biomarker-evaluable patients. Abbreviations: CXCL10, C-X-C motif chemokine ligand 10; G-MDSC, granulocyte-like myeloid-derived suppressor cells; NSCLC, non-small cell lung cancer; Nsq, nonsquamous; sq, squamous; sVEGFR2, soluble vascular endothelial growth factor receptor 2; VEGFA, vascular endothelial growth factor A.



## Results

### Patient Baseline Characteristics

- Baseline characteristics were generally balanced between the biomarker-evaluable population and the overall population (Table 1)

### Pharmacodynamic Biomarker Changes Post Treatment

- Changes in individual biomarker levels were consistent from C1D1 to both C2D1 and C3D1 (Figures 1 and 2), with
  - significant increases (*P*<0.0001 at both timepoints) for VEGFA, C-X-C motif chemokine ligand 10 (CXCL10) and IL-18
  - significant decreases across sVEGFR2 (*P*<0.0001; both timepoints), peripheral G-MDSCs (*P*=0.0005; *P*=0.0002), and monocytes (*P*<0.0001; both timepoints)
- Estimated fold changes of pharmacodynamic biomarkers were consistent across tumor types (Figure 3)

## References

- Du W, et al. *JCI Insight*. 2018;3:e124184.
- Zhang T, et al. *Cancer Immunol Immunother*. 2018;67:1079-1090.
- Shen L, et al. *J Immunother Cancer*. 2020;8:e000437.
- Zhao J, et al. *J Immunother Cancer*. 2023;11:e006055.

## Acknowledgments

This study is sponsored by BeiGene, Ltd. Medical writing support for the development of this poster, under direction of the authors, was provided by Yee Theng Soo, MSc, of Ashfield MedComms, an Inizio company, and was funded by BeiGene, Ltd. Editorial support was provided by Elizabeth Hermans, PhD, of BeiGene, Ltd.

## Disclosures

Jeffrey C Goh reports speaker fees from GSK and MSD; institutional, non-financial speaking engagement for Brisbane Cancer Conference; speaker's bureau participation for AstraZeneca, Eisai, GSK, Ipsen, Janssen, and MSD; advisory board participation for AstraZeneca, BMS, GSK, Janssen, and MSD; employment by ICON Chermiside & Greenslopes and Royal Brisbane & Women's Hospital (part time); stocks/shares for ICON Cancer Centres and Immunet; project lead for ITTACc trial (ceased); principal investigator for multiple pharma sponsored trials; member of ANZGOG, ANZUP, ASCO, and ESMO; leadership role as a member of ICON Cancer Centre Medical Advisory Committee.